On the uncertainties of the central density in axisymmetric galaxies resulting from deprojection

Bosch, F.C. van den

Mon. Not. R. Astron. Soc. **287,** 543–555 (1997)

On the uncertainties of the central density in axisymmetric galaxies resulting from deprojection

Frank C. van den Bosch★
Sterrewacht Leiden, Postbus 9513, 2300 RA Leiden, The Netherlands

Accepted 1997 January 3. Received 1996 October 30; in original form 1996 July 22

ABSTRACT

The deprojection of the surface brightness of axisymmetric galaxies is indeterminate unless the galaxy is seen edge-on. In practice, this problem is often circumvented by making ad hoc assumptions about the density distribution. However, one can redistribute the density and still project to the same surface brightness. This is similar to adding so-called konus densities to the assumed density distribution.

In this paper we investigate the maximum konus density that one can add to elliptical galaxies. In particular we focus on the uncertainties in the central densities of axisymmetric, elliptical galaxies arising from the non-uniqueness of the deprojection.

For Stäckel potentials a sufficient condition for positivity of the phase-space distribution function exists, which is used as a criterion for determining the maximum konus density that one can add to a perfect oblate spheroid. For small inclination angles we find an uncertainty in the central density of up to a factor 2.

Elliptical galaxies in general have a central density cusp. We therefore also investigate the maximum konus densities of cusped ellipticals. For these models we use an approximate criterion, which we have tested on the perfect oblate spheroid models. For sufficiently small scalelengths, the central density of the maximum konus density that can be added to a cusped elliptical is very high. In order to estimate the dynamical influence of konus densities on the central region, we calculate the mass fraction $M_{\rm kon}/M_{\rm gal}$ they can add to the centre. We show that this mass fraction is at most a few per cent. We also investigate the dynamical effect of cusped konus densities that have $\rho(r) \propto r^{-\alpha}$ at small radii. We show that konus densities can only be moderately cusped ($\alpha < 1$), and that an increase in cusp slope α results in a *decrease* of the mass fraction added to the centre by the konus density.

We illustrate all this by the specific example of M32, and show that the uncertainty in the central mass due to deprojection is negligible compared with the inferred mass of the central black hole (BH) in this galaxy.

Key words: galaxies: elliptical and lenticular, cD – galaxies: fundamental parameters – galaxies: individual: M32 – galaxies: kinematics and dynamics – galaxies: nuclei – galaxies: photometry.

1 INTRODUCTION

In recent years considerable progress has been made in the construction of axisymmetric dynamical models of galaxies (e.g., de Zeeuw 1994). Comparison of such models with observed kinematics has resulted in strong indications for the presence of a nuclear black hole (BH) in a number of galaxies (e.g., Kormendy & Richstone 1995). In order to construct such models one needs to recover the density distribution from the observed surface brightness distribution. However, Rybicki (1986) showed, by use of the Fourier slice theorem, that the deprojection of axisymmetric bodies is indeterminate unless the inclination angle $i = 90°$ (i.e., the galaxy is seen edge-on). In practice this problem is often circumvented by making an ad hoc assumption about the density distribution, e.g., considering only densities stratified on similar concentric ellipsoids. However, the Fourier slice theorem shows that any density distribution whose Fourier transform is only non-zero inside a cone with half-opening angle $90° - i$ and aligned with the symmetry axis of the Fourier transform of the density distribution (the so-called 'cone of ignorance') projects to zero surface brightness. Following the nomenclature of Gerhard & Binney (1996, hereafter GB) we will call such densities 'konus densities'. Franx (1988) gave an example of such a konus density which, when added to a triaxial Stäckel model, projects to zero surface brightness. GB investigated

★E-mail: vdbosch@strw.LeidenUniv.nl

the effect of adding or subtracting a specific family of konus densities $\rho_k(R,z|i_0)$ to a density distribution stratified on similar concentric ellipsoids $\rho_0(R,z)$. Although all densities

$$\rho(R,z) = \rho_0(R,z) + f\,\rho_k(R,z|i_0) \tag{1.1}$$

project to the same surface brightness if $i \leq i_0$, the underlying density distributions (and therefore the corresponding dynamics) can differ considerably.

In this paper we investigate to what extent one can add or subtract konus densities. In particular we focus on the uncertainty of the central density of axisymmetric galaxies due to the non-uniqueness of the deprojection. The kinematical evidence for the presence of nuclear BHs arises from the finding that the central density is too low in order to explain the observed kinematics. This density distribution is generally derived from the deprojection of the observed surface brightness, which requires assumptions on the inclination angle and the density distribution itself (i.e., the density is stratified on similar concentric ellipsoids). We apply our analysis to M32, in which the presence of a BH has been claimed. The mass of the BH that is inferred is of the order of 20 per cent of the total mass inside 1 arcsec. We investigate whether adding konus densities can redistribute the central mass such that we can elude the requirement of a BH in M32. We show that, although the maximum konus density that one can add can have very high central density (the konus density can even be cusped), the actual mass it adds to the nucleus (and therefore its dynamical influence) is negligible compared with the inferred BH.

This paper is organized as follows. In Section 2, we describe the criterion we use to determine the maximum konus density one can add to a certain galaxy model. Section 3 deals with the specific konus densities we use for our investigation. In Section 4 we discuss the uncertainties of the central density due to the freedom one has in redistributing the density distribution. In Section 5 an approximate criterion is discussed, which is applied to cusped galaxy models in Section 6. We discuss the application of all this to the specific example of M32 in Section 7. Finally, in Section 8, we summarize and discuss our results.

2 THE CRITERION

Since konus densities have regions of both positive and negative density there is an $f_{\rm max}$ such that for $f > f_{\rm max}$ there will be regions where the total density $\rho = \rho_{\rm gal} + f\rho_{\rm kon}$ is negative. Therefore, $f_{\rm max}$ expresses the maximum konus density under the physical criterion that $\rho > 0$. However, this criterion ignores whether or not such a galaxy can actually be built from its orbit building blocks. In general, for $f = f_{\rm max}$ there will be points $(R_0, |z_0|)$ in the meridional plane with zero density. It is easily seen that such models can not be physical. Orbits in an axisymmetric potential densely fill a limited area inside their zero-velocity curve. For thin tube orbits, this area shrinks to a one-dimensional curve. Let those curves be described by $\zeta(R,z)$ and parametrized by ϕ, such that $\phi = a$ in the equatorial plane and $\phi = b > a$ along the symmetry axis $R = 0$. It is easily seen that it is impossible to construct a model that has only one point in the first quadrant of the meridional plane $(R_0, z_0) \equiv (\zeta_0, \phi_0)$ with zero density, and $\rho > 0$ everywhere else. This is illustrated graphically in Fig. 1, where three orbits are plotted in the meridional (R,z) plane. The thick, solid curve is the curve with $\zeta = \zeta_0$, and the solid dot is the point (ζ_0, ϕ_0). As can be seen, all three plotted orbits are just allowed since they 'avoid' the solid dot, and therefore do not contribute density to (ζ_0, ϕ_0). Each orbit that contributes density to a point (ζ_0, ϕ'), with $\phi' > \phi_0$, also contributes density to all points $(\zeta_0, \phi < \phi')$. As a consequence, the only way to distribute orbits so that $\rho(\zeta_0, \phi_0) = 0$ is by having zero density along the entire curve with $(\zeta_0, \phi > \phi_0)$.

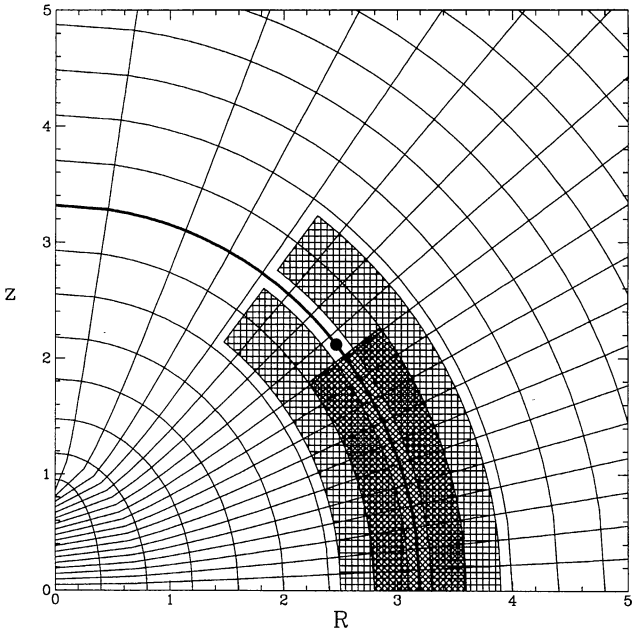

Figure 1. The grid shows curves of constant ζ and ϕ, which are the curves in between which orbits in an axisymmetric potential are enclosed. The hatched regions are three such orbits. The thick, solid curve is the curve with $\zeta = \zeta_0$ and the solid dot is the point (ζ_0, ϕ_0) (see text). As can be seen, having zero density in (ζ_0, ϕ_0) results in zero density along the entire curve $\zeta = \zeta_0$ with $\phi > \phi_0$.

In general this criterion is difficult to quantify. For Stäckel potentials, however, the third integral is known analytically and (ζ, ϕ) are the prolate spheroidal coordinates (λ, ν) (see Appendix A). Bishop (1987) formulated the principle outlined above by proving that a sufficient condition for the distribution function $f(E, L_z, I_3)$ of a Stäckel model to be non-negative and hence to correspond to a proper equilibrium model is that the density should monotonically decrease along lines of constant λ, i.e.,

$$\frac{\partial \rho(\lambda,\nu)}{\partial \nu} < 0. \tag{2.1}$$

In principle, one can still build physical models [i.e., $f(E, L_z, I_3) > 0$] that do not obey criterion (2.1), since it ignores the fact that orbits do not distribute density uniformly over the area in the (λ, ν) plane occupied by that orbit. The criterion, although sufficient, is therefore not strict, and will lead to an underestimate of the maximum konus density that can be added to a Stäckel potential.

As a specific example of a Stäckel model we will focus on the perfect oblate spheroids (see Appendix A), and use criterion (2.1) to investigate the maximum konus density one can add to such a density distribution. We note that if one adds a konus density to a Stäckel potential it is no longer a Stäckel potential, and therefore the orbits will no longer be confined by curves of constant λ and ν. However, as a first-order approximation, we can still use criterion (2.1). As we will show, the results presented in this paper are only mildly dependent on the actual curve along which we demand the gradient of the density to be negative (see Section 5).

3 THE KONUS DENSITY

In the following we will concentrate on ellipticals that have a luminous density that decays as r^{-4}. The surface brightness of such systems falls off as R^{-3} at large radii, which is in good agreement with observations. In order for the total density, $\rho = \rho_{\rm gal} + f\rho_{\rm kon}$, of such systems to be positive, we require a konus density that falls off as r^{-p} at large radii, where $p > 4$.

Furthermore, since we use the criterion that

$$\frac{\partial\rho}{\partial\nu} = \frac{\partial\rho_{\rm gal}}{\partial\nu} + f\,\frac{\partial\rho_{\rm kon}}{\partial\nu} < 0, \tag{3.1}$$

and since for the perfect oblate spheroid

$$\lim_{\lambda\to\infty}\frac{\partial\rho}{\partial\nu}(\lambda,\nu) \propto \lambda^{-2} = r^{-4}, \tag{3.2}$$

we require a konus density whose derivative with respect to the prolate spheroidal coordinate ν decays faster than r^{-4}.

The specific konus density introduced by GB (their equation 19) does not satisfy this criterion. We therefore seek another konus density. Kochanek & Rybicki (1996, hereafter KR) have developed a scheme to derive konus densities with a large variety of properties through the introduction of 'semi-konus densities'. A semi-konus density is a density that is non-zero in only one of the two halves of the cone of ignorance; either the cone at positive or at negative $\hat{z}$ (here $\hat{z}$ denotes the symmetry axis in Fourier space). Semi-konus densities are complex functions and KR showed that the real part of any semi-konus density is a konus density. Furthermore, semi-konus densities have the nice property that they are closed under ordinary multiplication: the product of two semi-konus densities is itself a semi-konus density. In particular any power

$$\rho^n(R,z) = \Re\left[\rho^1_{\rm sk}(R,z)\right]^n, \tag{3.3}$$

where $\Re$ denotes the real part, is a konus density as long as $\rho^1_{\rm sk}(R,z)$ is a semi-konus density. We will refer to konus densities of the form (3.3) as konus densities of order n.

We have experimented with several konus densities and finally came up with what we will refer to as the generalized konus density (see Appendix B). The generalized konus density is characterized by three parameters: a scalelength b, an order n, and an additional free parameter μ. Increasing the latter two increases the number of oscillations, as well as the power p of the decline at large radii. In order for the decline of both the density and the derivative (3.1) to be sufficiently fast we need to go to order $n \geq 6$. This is independent of μ. Throughout this paper we will mainly focus on the generalized konus densities with $\mu = 1$. A contour plot of this konus density with $n = 6$ in the meridional plane is shown in Fig. 2.

4 UNCERTAINTIES IN THE CENTRAL DENSITY

We now investigate the maximum konus density one can add to or subtract from a perfect oblate spheroid under the criterion of equation (2.1). We therefore seek the value

$$f_{\rm max} = \max(f_+, f_-), \tag{4.1}$$

where

$$f_\pm = \min_{(\lambda,\nu)}\left(f > 0; \frac{\partial\rho_{\rm gal}}{\partial\nu} \pm f\,\frac{\partial\rho^n_{\rm k}}{\partial\nu} = 0\right). \tag{4.2}$$

Here $\rho^n_{\rm k}$ is the nth order of the generalized konus density (see Appendix B). So f_+ describes the maximum konus density one can add, and f_- the maximum that can be subtracted. These are the minimal values of f for which the derivative of the total density with respect to ν equals zero. This value has to be searched over the entire (λ,ν) space. Once $f_{\rm max}$ is found we calculate

$$\Lambda_\nu \equiv \frac{f_{\rm max}\,\rho_{\rm k}(0,0|i)}{\rho_{\rm gal}(0,0)}. \tag{4.3}$$

The parameter Λ_ν therefore expresses the ratio of the central density of the maximum konus density over the central density of the perfect oblate spheroid.

The results for the generalized konus density of order 6 with $\mu = 1$ are presented in Fig. 3, where we plot the logarithm of Λ_ν as a function of the ratio b/a. Here b is the scalelength of the konus density and $a = \sqrt{-\alpha}$ is the break radius of the perfect oblate spheroid (see Appendix A). The results are shown for four different inclination angles ($i = 30°, 45°, 60°$ and $80°$), and two different flattenings ($q = 0.8$ and 0.5.) For small inclination angles the central density of the maximum konus density is of the same order of magnitude as the central density of the underlying spheroid (i.e., $\Lambda_\nu \approx 1$). However, that is only true if the scalelength of the konus density is approximately equal to the break radius of the perfect oblate spheroid (i.e., $b/a \approx 1$). For higher inclination angles, one can add less konus density to the model, reaching $f_{\rm max} = 0$ for $i = 90°$. We found that for $i = 80°$, the central density of the maximum konus density is no more than ~10 per cent of $\rho_{\rm gal}(0,0)$, and is such only if the scalelength of the konus density becomes small. In Fig. 4 we show how increasing μ or going to higher order n affects the maximum konus density. As can be seen, at $b/a \gtrsim 1$, the central density of the maximum konus density increases with both μ and n. For small scalelengths b, however, Λ_ν is maximal for the konus density with smallest μ and n (i.e., $\mu = 1, n = 6$). In fact the absolute maximum of Λ_ν is reached for the konus density with the smallest allowed values of μ and n.

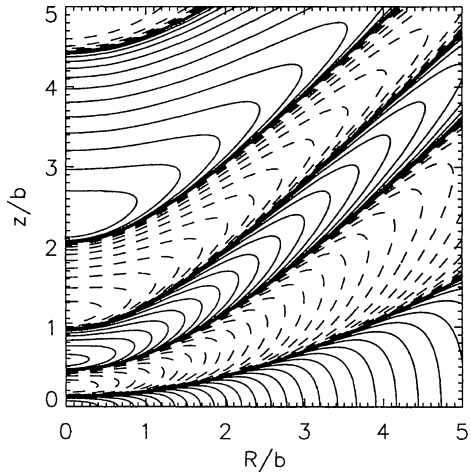

Figure 2. Contours of the 6th-order generalized konus density $\rho^6_{\rm k}(R,z|45°)$ for $\mu = 1$. This density distribution projects to zero surface brightness for $i \leq 45°$. Positive contours are solid, negative contours are dashed.

4.1 The luminosity profiles

Any konus density $\rho_{\rm k}(R,z|i_0)$ projects to zero surface brightness when seen under an inclination angle $i \leq i_0$. However, when a galaxy to which we add such a konus density is seen more edge-on

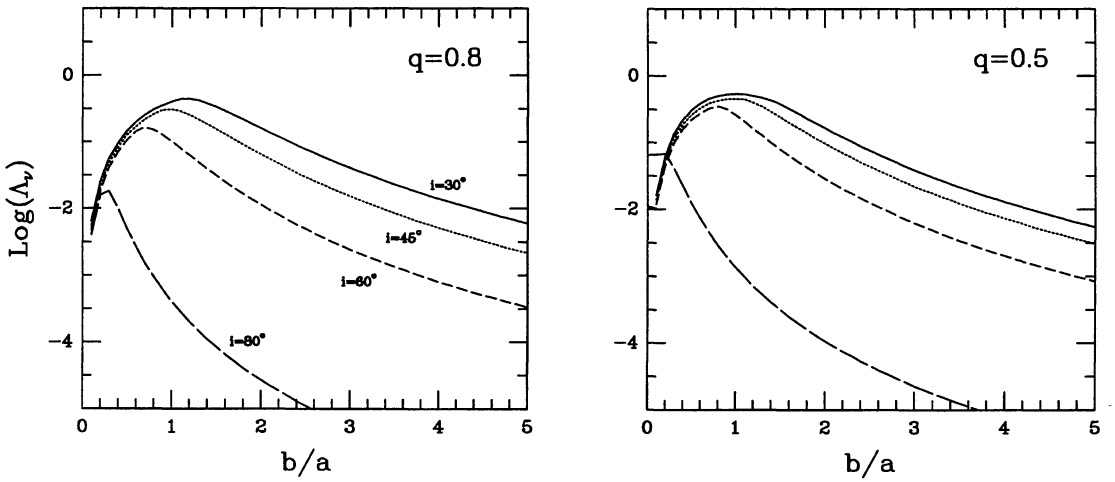

Figure 3. The logarithm of the parameter Λ_ν as a function of the ratio b/a for the 6th-order generalized konus density ($\mu = 1$). The results are presented for four different inclination angles: $i = 30°$ (solid lines), $i = 45°$ (dotted lines), $i = 60°$ (short-dashed lines), and $i = 80°$ (long-dashed lines). The panel on the left is for a perfect oblate spheroid with an ellipticity ϵ of 0.2, whereas the results in the panel on the right are for a model with $\epsilon = 0.5$.

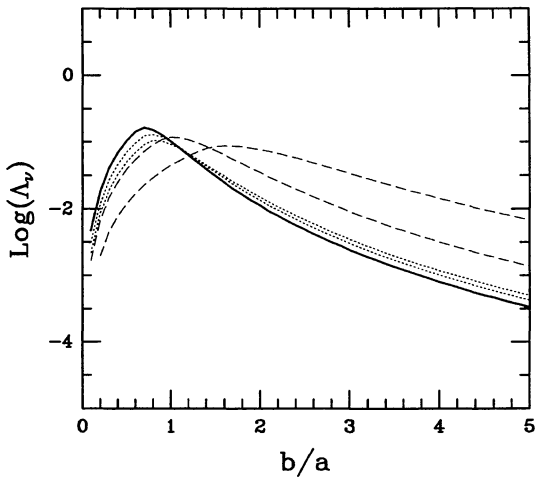

Figure 4. The same as Fig. 3, except that we now plot the maximum konus densities for different orders n of the generalized konus density and for different values of μ. All lines are for an oblate spheroid with $\epsilon = 0.2$, seen under an inclination angle of 60°. The thick, solid line is for $\mu = 1$ and $n = 6$. The dashed lines are for $\mu = 2$ and 4; and the dotted lines are for higher order, $n = 7$ and 8. As can be seen, the central density of the maximum konus density increases with both μ and n for large scalelengths b. However, for small scalelengths ($b/a \lesssim 1$), Λ_ν is highest for $\mu = 1$, $n = 6$.

($i > i_0$), it does *not* remain invisible. In order to examine how realistic galaxy models are with a maximum konus density, we project a perfect oblate spheroid with a maximum konus density $\rho_k(R, z|30°)$ under an inclination angle of 90° (i.e., we observe this galaxy edge-on), and compare the luminosity profiles along the major and minor axes with and without the maximum konus density. The results are shown in Fig. 5, where we plot the logarithm of the projected density versus the logarithm of the radius from the centre projected on the sky R. We plot the luminosity profiles along the major and minor axes. We consider the $\mu = 1$, $n = 6$ konus density with $b/a = 1.3$. For this ratio of the characteristic lengths a maximum value of Λ_ν was found (see Fig. 3).

As can be seen the presence of the (maximum) konus density is clearly visible. Its presence introduces wiggles in the luminosity profile along the minor axis. Galaxies with wiggles in their luminosity profiles are known. However, in all such cases the wiggles are mainly visible along the *major* axis profiles. Examples of such cases are galaxies that have embedded nuclear discs (see e.g., Ferrarese et al. 1994; van den Bosch, Jaffe & van der Marel 1997). The konus densities used here, however, reveal themselves by the presence of wiggles along the minor axis only. Since no such galaxies are known to exist, we can use this as an empirical criterion on the maximum konus density. We can make this criterion more qualitative by defining a maximum amplitude of the wiggle along the minor axis luminosity profile. We define the maximum konus density, according to the empirical criterion, as that konus density for which

$$\max_R |\mu_{\rm gal} - \mu_{\rm tot}| = 0.05, \qquad (4.4)$$

i.e., for which the maximum difference between the luminosity profiles with ($\mu_{\rm tot}$) and without ($\mu_{\rm gal}$) konus density is 0.05 mag. Given the photometric accuracy with which luminosity profiles can be measured observationally, any wiggle with an amplitude bigger than 0.05 mag should be detectable. In Fig. 6 we plot the maximum konus density Λ_ν that can be added to a perfect oblate spheroid with $q = 0.8$ as derived by using three different criteria: $\rho > 0$ (solid lines), $\partial\rho/\partial\nu < 0$ (dashed lines), and the empirical criterion (4.4) that the minor axis surface brightness profile, when projected edge-on, should not have wiggles bigger than 0.05 mag (dotted lines). The results are shown as a function of b/a for two different inclination angles ($i = 30°$ and 60°). In almost all cases the $\partial\rho/\partial\nu < 0$ criterion is dominant. Only for low inclinations, and $b/a \sim 1$–3, is the empirical criterion more strict.

5 AN APPROXIMATE CRITERION

Observations with the *Hubble Space Telescope* (*HST*) have revealed that all elliptical galaxies have central cusps in their density distribution (e.g., Ferrarese et al. 1994; Lauer et al. 1995). The perfect oblate spheroid we have studied so far has a density distribution that becomes constant inside its break radius $a = \sqrt{-\alpha}$, and therefore is not a realistic model for an elliptical galaxy. The advantage, however, of the perfect oblate spheroid is that it is a Stäckel potential, therefore we can use the criterion

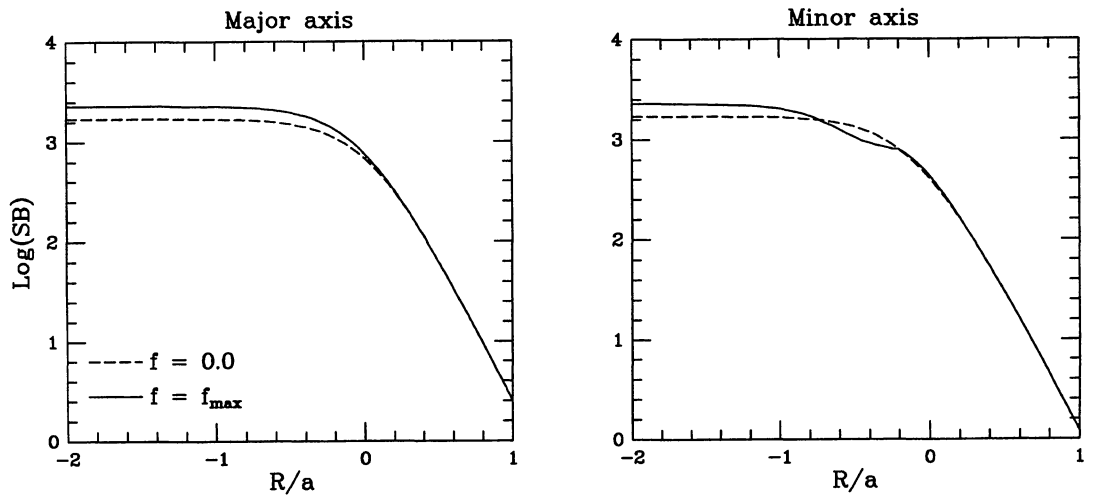

Figure 5. The luminosity profiles along the major and the minor axes of a perfect oblate spheroid with intrinsic flattening $q = 0.8$ seen edge-on (dashed lines). In addition, we also plot the luminosity profile of the same spheroid but to which we add the maximum konus density $\rho_k^6(R, z|30°)$. The scalelength of the konus density $b = 1.3a$, where a is the break radius of the spheroid. We have plotted the logarithm of the projected surface brightness (in arbitrary units) versus the logarithm of the radius on the sky R in units of a.

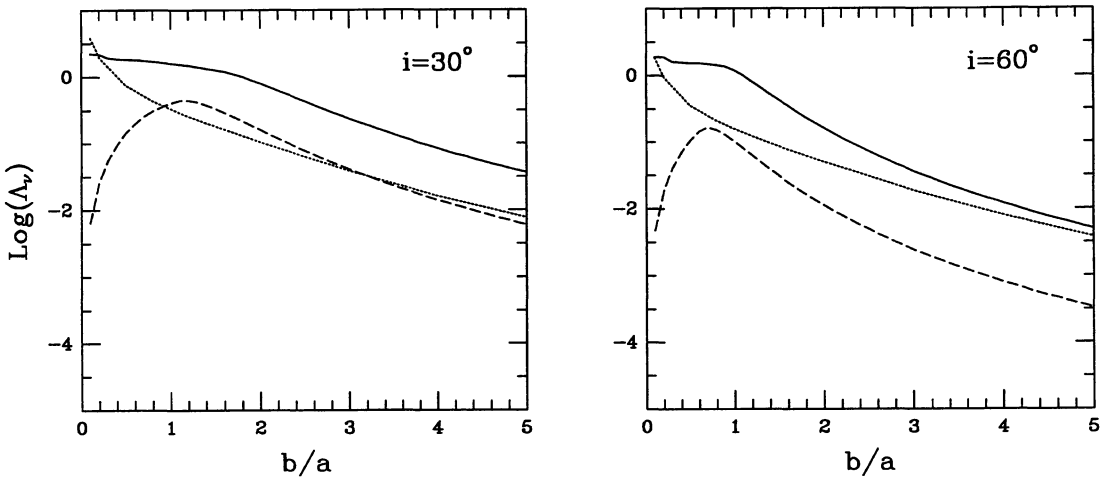

Figure 6. The maximum amount of konus density Λ_ν that can be added to a perfect oblate spheroid with $q = 0.8$, as determined from three different criteria: $\rho > 0$ (solid lines), $\partial\rho/\partial\nu < 0$ (dashed lines), and the empirical criterion that the minor axis surface brightness profile should not have wiggles (dotted lines). The results are shown as functions of b/a for two different inclination angles ($i = 30°$, and 60°).

$\partial\rho/\partial\nu < 0$. Unfortunately, no cusped Stäckel models are known. In order to investigate the uncertainty in the central density of realistic, centrally cusped, elliptical galaxies, we therefore need to use another criterion.

We use the criterion that the derivative of the total density distribution along a circular curve with radius $r = \sqrt{R^2 + z^2}$ has to be negative:

$$\frac{\partial\rho}{\partial\theta} < 0, \tag{5.1}$$

where $\theta = \arctan(z/R)$. We examine the accuracy of this approximate criterion, by comparing the values of Λ that we find for the perfect oblate spheroid using both the proper criterion (Λ_ν) and the approximate criterion (Λ_θ). The results are shown in Fig. 7, where we plot the ratio $\Lambda_\nu/\Lambda_\theta$ as a function of b/a for two different flattenings of the underlying perfect oblate spheroid ($q = 0.8$ and 0.5), and three different inclination angles ($i = 30°$, 60° and 80°). The approximate criterion always leads to an overestimate of the maximum konus density. The error is larger for smaller scalelengths b of the konus density, for smaller inclination angles, and for less flattened galaxies.

That criterion (5.1) leads to reasonably accurate approximations of the maximum konus density for the perfect oblate spheroid by no means ensures that it remains reasonable for, for instance, cusped galaxies. In fact, the finding that the approximate criterion leads to very accurate maximum konus densities when the scalelength is large is somewhat trivial given that at large radii the prolate spheroidal coordinate ν becomes equal to θ. Nevertheless, since the approximate criterion enforces a certain smoothness on the density distribution, we feel confident that this criterion will lead to more accurate maximum konus densities than simply using the criterion that the density has to be positive. We showed in Section 2 that under that naive criterion, one will overestimate the maximum konus densities (see also Fig. 6). In Section 7 we show that the

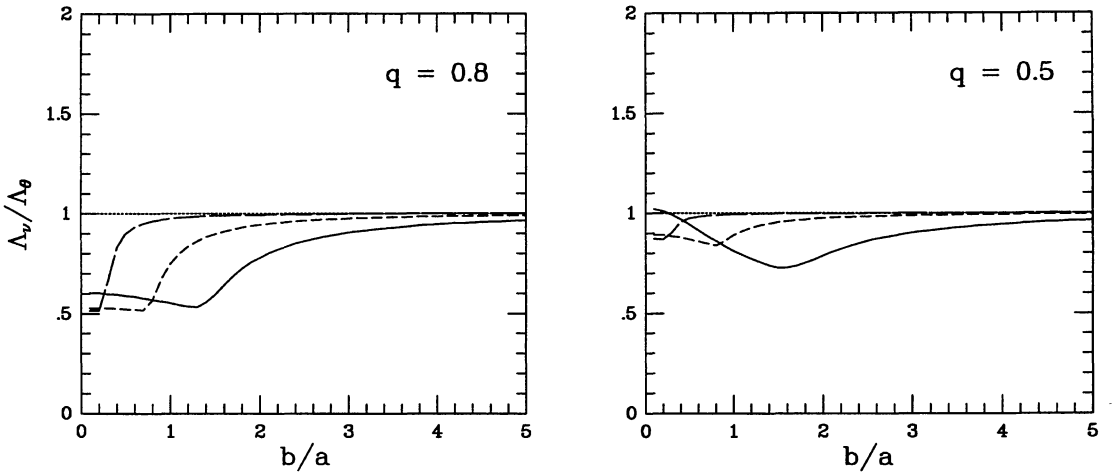

Figure 7. The ratio $\Lambda_\nu/\Lambda_\theta$ as function of the ratio b/a of the 6th-order generalized konus density ($\mu = 1$). The results are presented for three different inclination angles: $i = 30°$ (solid lines), $i = 60°$ (short-dashed lines) and $i = 80°$ (long-dashed lines). The panel on the left is for a perfect oblate spheroid with an ellipticity of 0.2, whereas the results in the panel on the right are for a model with $\epsilon = 0.5$.

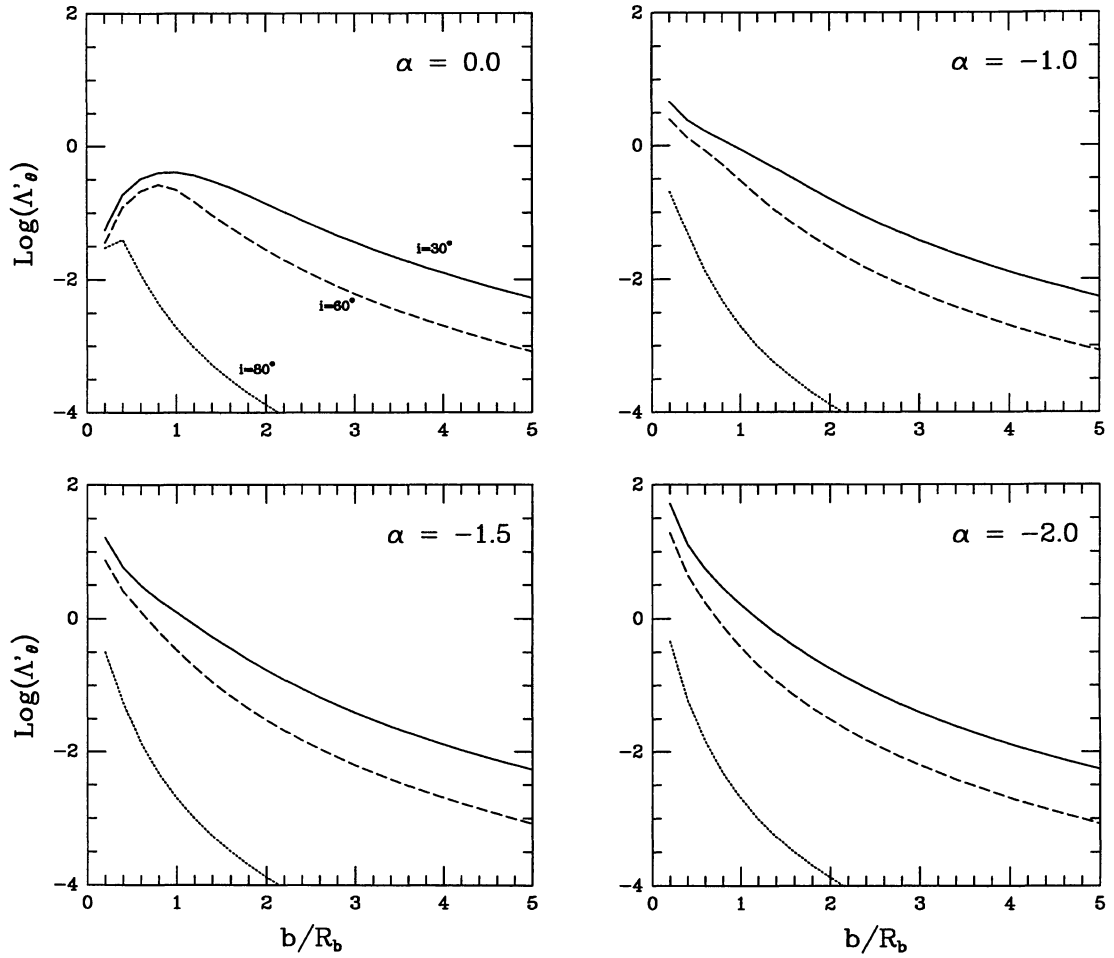

Figure 8. The ratio Λ'_θ of the central density of the maximum konus density over the density of the (α, β) model at its core radius R_b as function of the ratio b/R_b. Results are plotted for four different values of the cusp steepness α, and for three different inclination angles: $i = 30°$ (solid lines) $i = 60°$ (dashed lines) and $i = 80°$ (dotted lines). The maximum konus density increases strongly with increasing cusp steepness and decreasing konus scalelength b.

approximate criterion leads to similar maximum konus densities to the empirical criterion (4.4).

6 CUSPED DENSITY DISTRIBUTIONS

We now investigate the maximum konus density one can add to a cusped density distribution. We consider the so-called (α, β) models, which have proven to be useful representations of elliptical galaxies (e.g., Qian et al. 1995). The density distribution, which is given by

$$\rho(R,z) = \rho_0 \left(\frac{m}{R_b}\right)^{\alpha} \left[1 + \left(\frac{m}{R_b}\right)^2\right]^{\beta}, \tag{6.1}$$

is stratified on concentric ellipsoids $m = \sqrt{R^2 + z^2/q^2}$ of constant flattening q. For $R \gg R_b$ they fall off as $m^{\alpha+2\beta}$, while for $R \ll R_b$ they have $\rho \propto m^{\alpha}$. We will restrict ourselves to models that have $\alpha + 2\beta = -4$ so that at large radii their projected surface brightness falls off as R^{-3}.

We use the approximate criterion to investigate the dependence of the maximum konus density we can add to the density distribution of equation (6.1), as function of the cusp steepness α. We consider a strongly flattened galaxy ($q = 0.5$) seen under three different inclination angles ($i = 30°$, $60°$ and $80°$). When the cusp steepness $\alpha < 0$ the central density of the (α, β) model is infinite. We therefore cannot calculate the uncertainty of the central density Λ_θ. Instead, we calculate the ratio Λ'_θ of the central density of the maximum konus density over the density ρ_0 of the (α, β) model. We restrict ourselves to a konus density with $\mu = 1$ and $n = 6$. The results are shown in Fig. 8. When no cusp is present (i.e., $\alpha = 0$) we again find a maximum Λ'_θ at $b/R_b \sim 1$. However, for density distributions that are cusped we find that Λ'_θ keeps increasing when $b/R_b \rightarrow 0$. In the following section we will investigate the importance of this for galaxies where strong indications are found for the presence of a nuclear BH by discussing a specific example; the compact elliptical M32.

7 APPLICATION TO M32

To illustrate the importance of konus densities to real galaxies we here apply our analysis to M32. Strong evidence exists that M32 harbours a nuclear BH of $\sim 1.8 \times 10^6$ $M_\odot$ (van der Marel et al. 1994; Qian et al. 1995; Dehnen 1995). This evidence is based on the observations of a strong central increase of the velocity dispersion. In this section we investigate whether redistributing the central mass of M32 according to the konus density distribution can account for this increase without adopting the presence of a nuclear BH.

Although the inner part of the galaxy can accurately be described by an (α, β) model, this does not fit the outer parts of the galaxy. Multiplication of the (α, β) model with an additional factor can adequately describe the strong decrease of the density beyond $\sim$20 arcsec. We therefore follow the approach taken by van der Marel et al. (1997), and describe the density distribution of M32 by the following formula [hereafter referred to as an (α, β, γ) model]:

$$\rho(R,z) = \rho_0 \left(\frac{m}{R_b}\right)^{\alpha} \left[1 + \left(\frac{m}{R_b}\right)^2\right]^{\beta} \left[1 + \left(\frac{m}{R_c}\right)^2\right]^{\gamma}. \tag{7.1}$$

Projection of this density distribution and fitting to the observed surface brightness (from both *HST* and ground-based data) results in a good fit to the data for the parameters: $\alpha = -1.435$, $\beta = -0.423$, $\gamma = -1.298$, $R_b = 0.55$ arcsec, and $R_c = 102.0$ arcsec (van der Marel, private communication). Throughout we will assume a distance to M32 of 700 kpc, so that 1 arcsec corresponds to 3.4 pc.

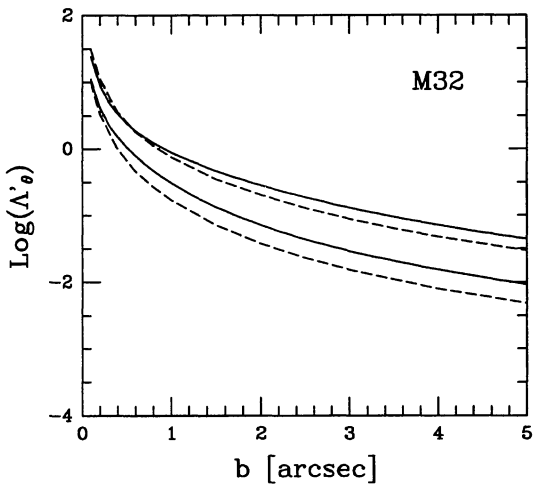

Figure 9. The logarithm of the parameter Λ'_θ as a function of the scalelength b of the generalized konus density for the (α, β, γ) model of M32. The lower two curves are for the konus density with $\mu = 1$ and $n = 6$, whereas the upper two curves correspond to a $\mu = 4$, $n = 6$ konus density. Solid curves correspond to criterion (5.1), whereas the two dashed curves show the maximum konus density as derived from the empirical criterion (4.4). Both criteria give values for Λ of the same order of magnitude, with the empirical criterion being slightly more strict.

An important problem with M32 is the fact that the inclination angle is unknown. Van der Marel et al. (1994) constructed axisymmetric models of M32 for different assumptions of the inclination angle ($i = 90°$ and $50°$). After solving the Jeans equations they concluded that both models require the presence of a $\sim 1.8 \times 10^6$ $M_\odot$ BH in order to fit the observed velocity dispersions in the centre. If indeed M32 is observed edge-on there is no uncertainty in the deprojection of the surface brightness so that no konus density can be added. Here we will focus on the $i = 50°$ model for which van der Marel et al. (1994) derived a mass-to-light ratio in the Johnson V band of 2.36. Given that the observed flattening of M32 is equal to 0.73, this results in an intrinsic flattening of the ellipsoids m of 0.452 (if $i = 50°$). The density ρ_0 of equation (7.1) is 1.76×10^5 $M_\odot$ pc^{-3}.

We have calculated the maximum konus density ρ_k^n that we can add to this (α, β, γ) model of M32. Since at large radii $m \propto m^{\alpha+2\beta+2\gamma} \sim m^{-4.8}$, we again need $n \geq 6$. We use the approximate criterion $\partial\rho/\partial\theta < 0$, and calculate the parameter Λ'_θ for different values μ, n and b of the konus density. The results are shown in Fig. 9 for two different values of μ ($\mu = 1$ and 4, both with $n = 6$). Unlike with the perfect spheroid, Λ is larger for higher μ or n *for each value of the scalelength* b (compare Fig. 4). In principle, we can make Λ' arbitrarily large by going to small b and large n or μ.

In addition, we have determined the maximum konus density allowed according to the empirical criterion (4.4) that the edge-on projected surface brightness along the minor axis should not have wiggles exceeding 0.05 mag (dashed lines in Fig. 9). Both criteria give rather similar values for Λ, although the empirical criterion is more strict. This is evident from Fig. 10, where we plot the luminosity profiles for the (α, β, γ) model of M32 both with (solid lines) and without (dashed lines) the maximum konus as derived from the approximate criterion.

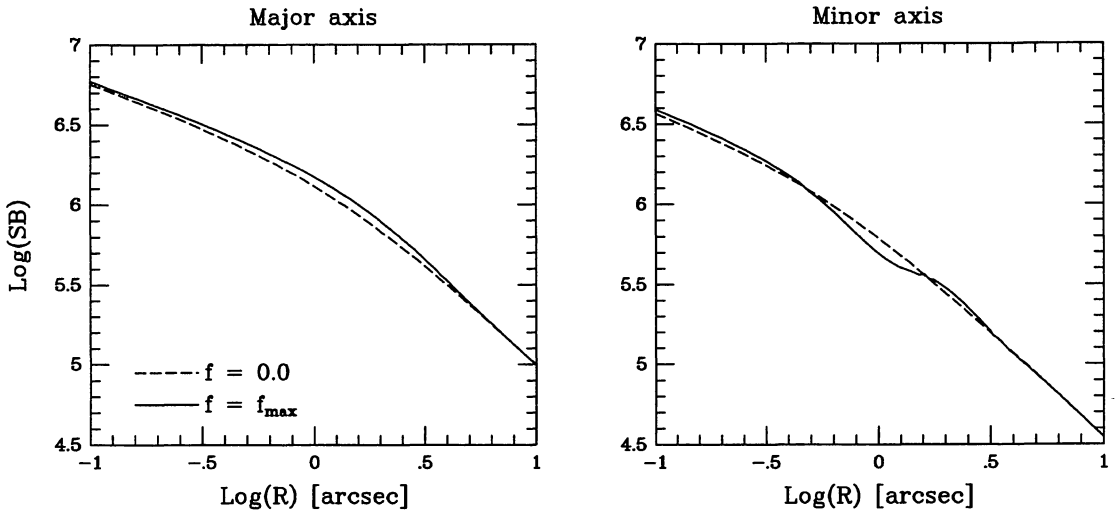

Figure 10. The logarithm of the edge-on projected surface brightness (in arbitrary units) of the (α, β, γ) model of M32, both with (solid lines) and without (dashed lines) the maximum konus density ($\mu = 1$, $n = 6$) derived from the approximate criterion.

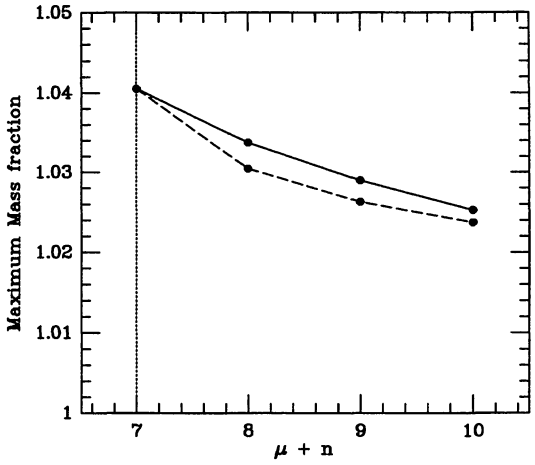

Figure 11. The maximum mass fraction $\Gamma_{\rm max}$ (equation 7.4) as a function of $\mu + n$. Since $\mu \geq 1$ and $n \geq 6$ we have a minimum $\mu + n = 7$. The solid line shows $\Gamma_{\rm kon}$ for increasing order n ($\mu = 1$), whereas the influence of increasing μ (with $n = 6$) is indicated by the dashed line.

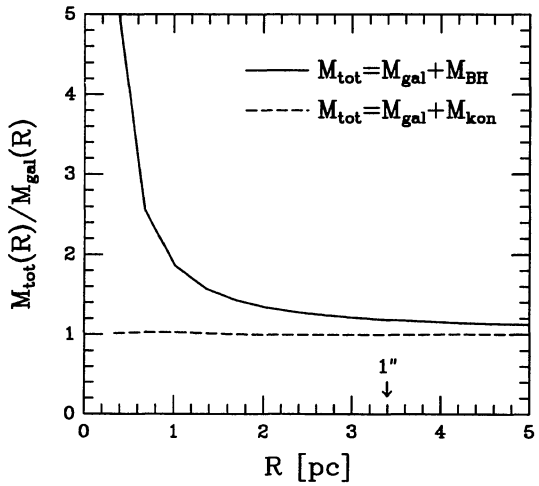

Figure 12. The total mass inside a sphere of radius R, $M_{\rm tot}(R)$, over the mass of the M32 density model inside the same sphere as function of radius R. The solid line shows the case in which the total mass is built up of the (α, β, γ) model of M32 with in addition a BH of 1.8×10^6 $M_\odot$. The dashed line is for the case in which we have added the maximum generalized konus density with $b = 1.0$ arcsec to the density model of M32.

7.1 Dynamical significance of konus densities

We have shown that by increasing μ or n we can make Λ' arbitrarily large. However, Λ' is the central konus density divided by the density of the galaxy at $m = R_b$. Since the central density of a cusped galaxy is by definition infinite, it is not a priori clear what the real, dynamical significance of these maximum konus densities is. In order to compare the dynamical significance of the (maximum) konus density with that of the inferred BH, we have calculated the ratios

$$\Gamma_{\rm BH}(r) = \frac{M_{\rm gal}(r) + M_{\rm BH}}{M_{\rm gal}(r)} \tag{7.2}$$

and

$$\Gamma_{\rm kon}(r) = \frac{M_{\rm gal}(r) + M_{\rm kon}(r)}{M_{\rm gal}(r)}. \tag{7.3}$$

Here $M(r)$ is the mass inside a sphere of radius r, and $M_{\rm gal}$ is the mass of the (α, β, γ) model. Although the total mass of the konus density is zero, at a sufficiently small radius there is only a positive density contribution resulting in a non-zero positive $M_{\rm kon}(r)$. Since the central konus density is finite, $\Gamma_{\rm kon}(r)$ is unity at $r = 0$, reaches a maximum at a certain intermediate radius, and decreases to unity again at larger radii. This $\max_r \Gamma_{\rm kon}(r)$ depends on the scalelength b of the konus density, as well as on μ and n. For each μ and n we calculate the maximum mass fraction, defined as

$$\Gamma_{\rm max} = \max_b[\max_r \Gamma_{\rm kon}(r)]. \tag{7.4}$$

This maximum mass fraction as function of $\mu + n$ is shown in Fig. 11. Although increasing $\mu + n$ increases the central density of the maximum konus density (see Fig. 9), the number of oscillations increases as well. Therefore, the central region where $\rho_{\rm k} > 0$ becomes smaller and we find that $\Gamma_{\rm max}$ *decreases* with increasing $\mu + n$. For our generalized konus density we find an absolute

maximum mass fraction of only ~1.04. This maximum is reached for a konus density with $b = 0.22$ arcsec, $\mu = 1$ and $n = 6$. It is not only important what the absolute mass fraction is, but also at what radius it is reached. In Fig. 12 we have plotted the radial run of Γ_{BH}. If $\Gamma_{max} = 1.04$ is reached at 5 pc, it is comparable to Γ_{BH}. However, the maximum mass fraction occurs at very small radii ($r \approx 0.7$ pc), where Γ_{BH} is many orders of magnitude larger. If the scalelength b of the konus density increases, the radius where $\Gamma_{kon}(r)$ is maximal increases, but since Λ decreases strongly with scalelength (Fig. 9) the maximum Γ_{kon} also decreases with b. We therefore conclude that the dynamical influence of the maximum generalized konus density is negligible compared with that of the inferred BH.

7.2 Cusped konus densities

The Fourier transform of the generalized konus density decays exponentially at large frequency k (see Appendix B). This enforces $\partial\rho_k/\partial r$ to go to zero at small radii r. Here we investigate whether konus densities with a central density cusp can add more mass to the centre. In order for a konus density to be cusped, i.e., $\rho_k \propto r^{-\alpha}$ ($0 < \alpha < 3$) at small radii, its Fourier transform should decay as $k^{\alpha-3}$ at large frequencies k. The requirement $\alpha < 3$ ensures that the density cusp has finite mass. We can constrain this regime even further by taking into account the fact that every konus density projects to zero surface brightness when projected face-on (i.e., with $i = 0°$). Since

$$\int_0^a r^{-\alpha} \mathrm{d}r = \infty, \tag{7.5}$$

for $\alpha \geq 1$ and $a > 0$, the projected surface brightness at the centre can only be equal to zero if $\alpha < 1$. Therefore, konus densities can at most be moderately cusped, with a central density gradient less steep than r^{-1}.

As we have seen in the previous section, maximizing Γ_{kon} not only requires high central density but also a sufficiently large area in the centre where $\rho_k > 0$. A cusped konus density with this property, in order to have zero total mass, must have regions outside the centre with strongly negative density. Addition of such a konus density is therefore likely to result in luminosity profiles (when projected edge-on) with large wiggles. In other words, it seems likely that the empirical criterion (4.4) becomes most strict. In fact, already for our generalized konus density, this criterion is the most restricting (see Fig. 9). In order to quantify this, we have tried to construct cusped konus densities, but were unable to find an analytical $\rho_k(R, z)$ that obeys the physical restrictions of konus densities, i.e., zero total mass, sufficiently rapid decay at large radii, and no discontinuities. We therefore constructed a density distribution that *resembles* a cusped konus density. Consider the density distribution

$$\rho_c(R, z|i) = \rho_0\, r^{-\alpha}\, \mathrm{e}^{-r/c}\, \mathrm{e}^{-R/b} \tanh\left(\frac{\sqrt{R^2 + d^2}\tan^{-1} i - z}{z}\right). \tag{7.6}$$

Here $r = \sqrt{R^2 + z^2}$, and α, b, c and d are free parameters. This density is cusped in the centre (with power-law slope α), and decays exponentially at large radii $r >> c$. At $z = \sqrt{R^2 + d^2}\tan^{-1} i$ the density changes sign, becoming negative at larger z. We adopt α and c as free parameters and use the physical properties of genuine konus densities to determine b and d. Since we have added the factor $\mathrm{e}^{-R/b}$, which equals unity for $z = 0$, we can use the requirement that the line-of-sight integral along the minor axis should yield zero, i.e.,

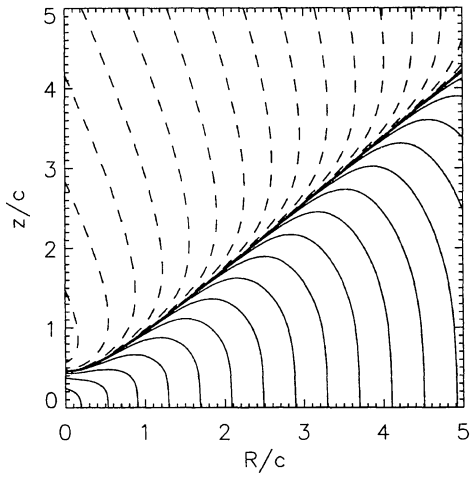

Figure 13. A contour plot of the cusped 'konus' density $\rho_c(R, z|50°)$ for $\alpha = 0.25$. The parameters b and d are taken such that $\rho_c(R, z|50°)$ obeys criteria (7.7) and (7.8).

$$\int_{-\infty}^{\infty} \rho_c(R = 0, z|i)\mathrm{d}z = 0, \tag{7.7}$$

to numerically evaluate the ratio d/c. Once d is known, we determine the ratio b/c by numerical evaluation of the root of

$$M_{tot} = 4\pi \int_0^{\infty} \mathrm{d}R\, R \int_0^{\infty} \mathrm{d}z\, \rho_c(R, z|i) = 0. \tag{7.8}$$

A contour plot of a cusped 'konus' density with $\alpha = 0.25$ that obeys these criteria is shown in Fig. 13. Although (7.6) is not a konus density, we can interpret it as such and use the empirical criterion (4.4) to determine the maximum 'konus' density. The empirical criterion uses the edge-on projected surface brightness along the minor axis, and along this axis (7.6) at least resembles a genuine cusped konus density, in that it obeys criterion (7.7). As we have seen for the generalized konus density, the maximum mass fraction decreases for an increasing number of density oscillations. Our cusped 'konus' density has a minimal number of density oscillations, and is therefore biased towards larger Γ_{kon}. We have calculated, as function of α and scalelength c, the $\max_r \Gamma_{kon}(r)$ for our cusped 'konus' density when added to M32. The results are shown in Fig. 14. As in the case of the generalized konus density, $\max_r \Gamma_{kon}(r)$ increases with decreasing scalelength. More importantly, increasing the cusp slope α *decreases* Γ_{kon}. This is due to the fact that for larger α the konus criterion (7.7) ensures that d decreases, so that the central region where $\rho_c > 0$ becomes smaller. Evidently, this effect is stronger than the increase in cusp slope. We therefore conclude that even cusped konus densities have a negligible dynamical effect on the central region of M32, as compared with that of the inferred BH mass. In the analysis above we have used a BH mass of $1.8 \times 10^6\ M_\odot$. More recent studies hint towards a more massive BH of $\sim 3 \times 10^6\ M_\odot$ (Bender, Kormendy & Dehnen 1996; van der Marel et al. 1997). This only strengthens the conclusions outlined above.

8 CONCLUSIONS

The deprojection of axisymmetric systems is indeterminate when the inclination angle $i \neq 90°$. To any such system one can add densities which, after projection, result in zero surface brightness.

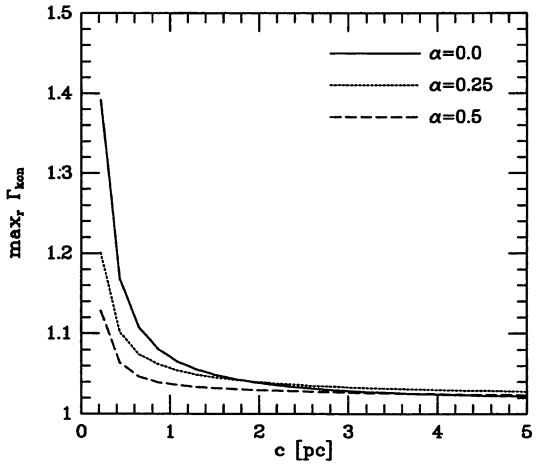

Figure 14. The maximum of $\Gamma_{\rm kon}$ over radius r for our cusped 'konus' density ρ_c (7.6) as a function of its scalelength c and cusp slope α. Increasing the cusp slope decreases the mass fraction added to the centre by the 'konus' density, therewith resulting in a smaller dynamical effect as compared with that of the BH.

Since these density distributions have zero total mass, addition or subtraction of konus densities is similar to redistributing the mass of the system. In this paper we have investigated to what extent one can redistribute the mass in elliptical galaxies. In particular, we investigated the uncertainties of the central densities of such galaxies due to the non-uniqueness of the deprojection.

Since konus densities have regions with both positive and negative density, there is a limit on how much konus density can be added to any density distribution while maintaining positivity. Although this criterion will result in a maximum konus density, it ignores whether a model with such a maximum konus density can actually be built from its orbit building blocks. We therefore use a more realistic (and more strict) criterion to determine the maximum konus density.

We used both a physical and an empirical criterion. The physical criterion is based on the principle that the density should be monotonically decreasing along curves that follow thin tube orbits. This criterion, although sufficient, is not strict. For Stäckel potentials, these thin tube orbits are described by the curves of constant prolate spheroidal coordinate λ, and the criterion can be made quantitative. For any other potential, no analytic description of the curves is known. In those cases we use an approximate criterion that states that $\partial\rho/\partial\theta < 0$ along circles of constant radius $r = \sqrt{R^2 + z^2}$ with $\theta = \arctan(z/R)$. The empirical criterion we used is based on the fact that adding too much konus density will result in wiggles along the minor axis luminosity profile, when the galaxy is seen edge-on. Since no such systems have ever been observed this puts an empirical constraint on the maximum konus densities.

We calculated the ratio of the central density of the maximum konus density to the central density of the perfect oblate spheroid to which that konus density can be added. For sufficiently small inclination angles, one can add konus densities whose central density is comparable to that of the perfect oblate spheroid. For highly inclined galaxies, the uncertainty of the central density is small, however: $\lesssim$10 per cent for $i \gtrsim 80°$. Perfect oblate spheroids have a break radius inside which the density is constant. Elliptical galaxies, however, are known to harbour central density cusps. We therefore applied the approximate criterion to cusped, axisymmetric models that have $\rho \propto r^{-\alpha}$ at small radii. The steeper the cusp the more konus density one can add. The central density of the maximum konus density increases strongly with decreasing scalelength of the konus density and with decreasing inclination angle.

In order to better understand the dynamical significance of maximum konus densities, we applied our analysis to the specific example of M32; a compact elliptical for which strong indications are found for the presence of a central BH of $\sim 2 \times 10^6\,{\rm M}_\odot$. The central density distribution of M32 is strongly cusped ($\rho \propto r^{-1.435}$), and we used both the approximate criterion and the empirical criterion to determine the maximum amount of konus density. The latter was found to be more strict. Although for sufficiently small scalelengths of the konus density its central density can be very large, its dynamical influence on the central region of M32 is negligible. This is due to the cusped nature of the central density distribution of M32.

We have also investigated the dynamical influence of *cusped* konus densities. We have shown, based on a simple argument, that konus densities can only be moderately cusped [$\rho_{\rm kon}(r) \propto r^{-\alpha}$ with $\alpha < 1$]. We were unable to find an analytic, cusped konus density, and therefore used a cusped density distribution that *resembles* a cusped konus density. We made sure that this density distribution has zero total mass and, when projected face-on, has zero surface brightness in the centre. Using the empirical criterion, we showed that for increasing cusp slope α, the mass fraction that the konus adds to the centre *decreases*. This is due to the fact that an increase in cusp slope results in a decrease of the central region where $\rho_{\rm kon} > 0$.

We conclude therefore that konus densities play only a marginally important role in the study of the dynamics of the central regions of (cusped) elliptical galaxies. Although considerable amounts of konus density can be added, when its scalelength is sufficiently small, its dynamical influence on the central dynamics remains negligible. In particular, we conclude that the uncertainties in the central mass of axisymmetric galaxies due to the non-uniqueness of the deprojection are sufficiently small that they cannot exclude the requirement of a central BH based on the finding of too small central densities in these galaxies. This is increasingly true in galaxies seen under larger inclination angles.

A major shortcoming in the investigations discussed in this paper is the fact that only one particular class of konus densities was used. However, the different free parameters of this generalized konus density allowed a wide range of konus densities to be investigated. Although the cusped 'konus' density distribution was not a real konus density, it obeyed at least two konus criteria, and we merely used it to investigate the *changes* in mass fraction when cusp slope is increased rather than to interpret the *absolute* mass fraction for this 'konus' density. We are therefore confident that the conclusions reached in this paper are at most very moderately dependent on our actual choice of konus densities used.

ACKNOWLEDGMENTS

The author would like to thank Nicolas Cretton, Walter Jaffe, Tim de Zeeuw and Roeland van der Marel for valuable discussions. In addition, the author is grateful to the referee, Dr P. L. Palmer, whose comments helped to improve the paper considerably. This research was financially supported by the Netherlands Foundation for Astronomical Research (ASTRON), #782-373-055, with financial aid from the Netherlands Organization for Scientific Research (NWO).

REFERENCES

Bender R., Kormendy J., Dehnen W., 1996, ApJ, 464, L123
Bishop J. L., 1987, ApJ, 322, 618
Dehnen W., 1995, MNRAS, 274, 919
de Zeeuw P. T., 1994, in Mũnoz-Tuñón C., Sánchez F., eds, The Formation and Evolution of Galaxies. Cambridge Univ. Press, Cambridge, p. 231
de Zeeuw P. T., Lynden-Bell D., 1985, MNRAS, 215, 713
Ferrarese L., van den Bosch F. C., Ford H. C., Jaffe W., O'Connell R. W., 1994, AJ, 108, 1598
Franx M., 1988, MNRAS, 231, 285
Gerhard O. E., Binney J. J., 1996, MNRAS, 279, 993 (GB)
Gradshteyn I. S., Ryzhik I. M., 1980, Table of Integral, Series, and Products. Academic Press, New York
Kochanek C. S., Rybicki G. B., 1996, MNRAS, 280, 1257 (KR)
Kormendy J., Richstone D., 1995, ARA&A, 33, 581
Kuzmin G. G., 1953, Tartu Astrophys. Obs. Teated, 1
Kuzmin G. G., 1956, AZh, 33, 27
Lauer T. R. et al., 1995, ApJ, 110, 2622
Qian E., de Zeeuw P. T., van der Marel R. P., Hunter C., 1995, MNRAS, 274, 602
Rybicki G. B., 1986, in de Zeeuw P. T., ed., Proc. IAU Symp. 127, Structure and Dynamics of Elliptical Galaxies. Kluwer, Dordrecht, p. 397
van den Bosch F. C., Jaffe W., van der Marel R. P., 1997, MNRAS, submitted
van der Marel R. P., Evans N. W., Rix H.-W., White S. D. M., de Zeeuw P. T., 1994, MNRAS, 271, 99
van der Marel R. P., Cretton N., Rix H.-W., de Zeeuw P. T., 1997, ApJ, submitted

APPENDIX A: THE PERFECT OBLATE SPHEROID

Kuzmin (1953, 1956) showed that there exists exactly one oblate potential for which the density is stratified on similar, concentric aligned spheroids, and for which the equations of motion are separable. This model has become known as the perfect oblate spheroid (de Zeeuw & Lynden-Bell 1985), and has a potential of Stäckel form, i.e.,

$$\Phi = -\frac{(\lambda+\gamma)G(\lambda)-(\nu+\gamma)G(\nu)}{\lambda-\nu}, \tag{A1}$$

where $G(\tau)$ is an arbitrary function ($\tau=\lambda,\nu$) and (λ,ϕ,ν) are prolate spheroidal coordinates, in which the equations of motion are separable. The coordinates λ and ν are defined as the roots for τ of

$$\frac{R^2}{\tau+\alpha}+\frac{z^2}{\tau+\gamma}=0, \tag{A2}$$

where R and z are the cylindrical coordinates, α and γ are negative constants, and we choose $-\gamma\le\nu\le-\alpha\le\lambda$. The foci of the coordinates are at $(R,z)=(0,\pm\Delta)$, with $\Delta^2=\gamma-\alpha$. The coordinates (R,z) can be written as

$$R^2=\frac{(\lambda+\alpha)(\nu+\alpha)}{\alpha-\gamma},\quad z^2=\frac{(\lambda+\gamma)(\nu+\gamma)}{\gamma-\alpha}. \tag{A3}$$

The density distribution of the perfect oblate spheroid is given by

$$\rho(R,z)=\rho_0\frac{a^4}{(a^2+m^2)^2}, \tag{A4}$$

where $a=\sqrt{-\alpha}$, and $m^2=R^2+z^2/q^2$ are the spheroids with flattening $q=\sqrt{\gamma/\alpha}$. The density distribution in the equatorial plane has a break radius at a. At radii $r>>a$ the density falls off as r^{-4} (consistent with the fact that the surface brightness of most galaxies falls off as approximately R^{-3}). At small radii ($r<<a$) the density is constant and equal to the central density ρ_0. The density distribution can be expressed in prolate spheroidal coordinates as

$$\rho(\lambda,\nu)=\rho_0\left(\frac{\alpha\gamma}{\lambda\nu}\right)^2. \tag{A5}$$

APPENDIX B: A GENERALIZED KONUS DENSITY

Here we follow the approach taken by KR, and consider the class of semi-konus densities which can be written as

$$\rho_{\rm sk}(R,z|i)=\frac{[f_{\rm s}(\alpha_+)+f_{\rm s}(\alpha_-)]}{r}-i\,\frac{[f_{\rm c}(\alpha_+)-f_{\rm c}(\alpha_-)]}{r}, \tag{B1}$$

where $\alpha_\pm=\sqrt{R^2+z^2}\cos i\pm z$, and $f_{\rm s}(x)$ and $f_{\rm c}(x)$ are odd and even functions, respectively, defined by

$$f_{\rm c}(x)=\frac{1}{4\pi^2}\int_0^\infty {\rm d}k\; g(k)\;\cos(kx) \tag{B2}$$

and

$$f_{\rm s}(x)=\frac{1}{4\pi^2}\int_0^\infty {\rm d}k\; g(k)\;\sin(kx). \tag{B3}$$

Upon choosing a weight function $g(k)\propto k^{\mu-1}{\rm e}^{-bk}$ one derives with the help of formulae 3.944.5 and 3.944.6 in Gradshteyn & Ryzhik (1980)

$$f_{\rm c}(x)=\frac{\Gamma(\mu)}{(b^2+x^2)^{\mu/2}}\cos\left[\mu\;\arctan\left(\frac{x}{b}\right)\right] \tag{B4}$$

and

$$f_{\rm s}(x)=\frac{\Gamma(\mu)}{(b^2+x^2)^{\mu/2}}\sin\left[\mu\;\arctan\left(\frac{x}{b}\right)\right], \tag{B5}$$

where $\Gamma(x)$ is the gamma function. These functions define a continuous class of konus densities $\rho_{\rm k}(R,z|i)=\Re\rho_{\rm sk}(R,z|i)$ for $\mu>0$. Here $\Re f$ denotes the real part of f. For $\mu=1$ the semi-konus density (B1) reduces to the first-order semi-konus density given by KR in their equation (20). In the following we will only consider integer values of μ.

In the limit $r=\sqrt{R^2+z^2}\to\infty$ the konus densities $\rho_{\rm k}(R,z|i)$ decline as $r^{-(\mu+1)}$ for μ odd and as $r^{-(\mu+2)}$ for μ even. This continuous set of konus densities therefore can be chosen to decline arbitrarily rapidly at large radii. In Fig. B1 we show contour plots for the cases with $\mu=1,2,3$ and 4. Note that for $\mu\ge3$ these konus densities also change sign in the equatorial plane.

As we prove in Appendix C, the generalized konus density $\rho^\mu_{\rm k}(r,z|i_0)$ with $\mu=1$ has infinite total mass. For $i<i_0$ it projects to constant, but *non-zero* surface brightness. Therefore, addition of such a konus density is no longer equivalent to simply redistributing the density. For $\mu=2$ the total mass is finite but positive, whereas for $\mu>2$ the total mass is zero (see Appendix C).

As was shown by KR, any function

$$\rho^n(R,z)=\Re[\rho^1_{\rm sk}(R,z)]^n \tag{B6}$$

is a konus density as long as $\rho^1_{\rm sk}(R,z)$ is a semi-konus density. KR have presented examples of such higher order konus densities for the case of $\mu=1$ of our generalized konus density.

As discussed in Section 3, in order to ensure that realistic axisymmetric galaxy models can be constructed with the addition or subtraction of konus densities, one needs konus densities that decline sufficiently fast. Any konus density of the form (B1), with $f_{\rm s}(x)$ odd [$f'_{\rm s}(0)\ne0$] and $f_{\rm c}(x)$ even [$f_{\rm c}(0)\ne0$], has $\rho^n_{\rm k}\propto r^{-n}$ for n even and $\partial\rho^n_{\rm k}/\partial\theta\propto r^{-(n-1)}$ for n odd along lines $\alpha_\pm=0$. Here

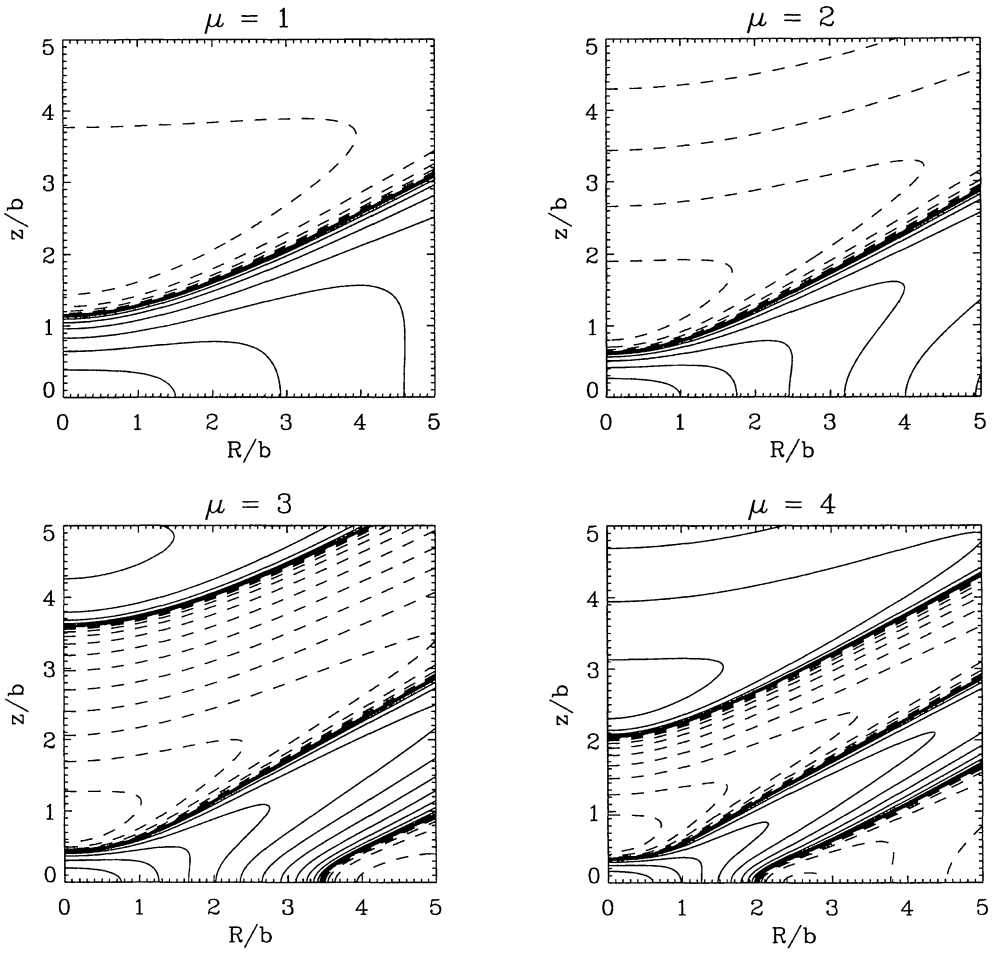

Figure B1. Contours of the generalized $\rho_k(R, z|60°)$ for $\mu = 1, 2, 3$ and 4. Each of these density distributions projects to zero surface brightness for $i < 60°$. Positive contours are solid, negative contours are dashed.

$\theta = \arctan(z/R)$, but the same is true for the derivative with respect to the prolate spheroidal coordinate ν. In order to have a konus density that declines faster than r^{-4} at large radii, and whose derivative $\partial\rho_k/\partial\theta$ declines faster than r^{-4}, we need to go to order $n \geq 6$. Besides a more rapid asymptotic decline for higher order n, the konus density will also show a greater number of sign alterations.

APPENDIX C: THE TOTAL MASS OF THE GENERALIZED KONUS DENSITIES

Let $H(\boldsymbol{k})$ be the Fourier transform of the semi-konus density $\rho_{sk}(r, z|\theta)$, where $\theta = 90° - i$. We will use spherical coordinates (k, ψ, ϕ) for the Fourier space vector $\boldsymbol{k}$. Then $H(\boldsymbol{k}) = H(k, \psi)$ since the Fourier transform of the semi-konus density is symmetric around the k_z axis. We follow the approach taken by KR and build up $H(\boldsymbol{k})$ by a weighted sum of kernel functions $f(\boldsymbol{k}, \boldsymbol{k}_0)$, i.e.,

$$H(\boldsymbol{k}) = \int_0^\infty \mathrm{d}k_0\, g(k_0) f(\boldsymbol{k}, \boldsymbol{k}_0). \tag{C1}$$

For our specific semi-konus density of the form (B1), the kernel is a shell of radius $|\boldsymbol{k}_0| = k_0$ shifted along the k_z axis by an amount $k_0/\sin\theta$, and

$$f(\boldsymbol{k}, \boldsymbol{k}_0) = \frac{\delta\big(|\boldsymbol{k} - \boldsymbol{k}_0/\sin\theta| - |\boldsymbol{k}_0|\big)}{|\boldsymbol{k}_0|}, \tag{C2}$$

where $\delta(x)$ is the delta function. This is illustrated in Fig. C1, where we have plotted the cone with half-angle θ in the meridional plane of $\boldsymbol{k}$. As can be seen, at any point (k, ψ, ϕ) (with $\psi < \theta$) there are two shells that contribute weight to that point. We define the function $f(k_0)$ as

$$\begin{aligned} f(k_0) &\equiv |\boldsymbol{k} - \boldsymbol{k}_0/\sin\theta| - |\boldsymbol{k}_0| \\ &= \sqrt{k^2 + \frac{k_0^2}{\sin^2\theta} - 2k\frac{k_0}{\sin\theta}\cos\psi} - k_0. \end{aligned} \tag{C3}$$

From the normalization relation of δ-functions we have that

$$\delta\big[f(k_0)\big] = \frac{\delta(k_0 - k')}{f'(k')}, \tag{C4}$$

where k' are those k_0 for which $f(k_0) = 0$. Solving $f(k_0) = 0$ we find two solutions $k' = k_\pm$:

$$k_\pm = k\frac{\sin\theta}{\cos^2\theta}\left(\cos\psi \pm \sqrt{\cos^2\psi - \cos^2\theta}\right). \tag{C5}$$

Calculating the derivative $f'(k_0)$ and using equations (C2), (C4) and (C5) we find (for $\psi < \theta$)

$$H(\boldsymbol{k}) = \frac{\sin\theta}{\sqrt{\cos^2\psi - \cos^2\theta}}\left[\frac{g(k_+)}{k} - \frac{g(k_-)}{k}\right]. \tag{C6}$$

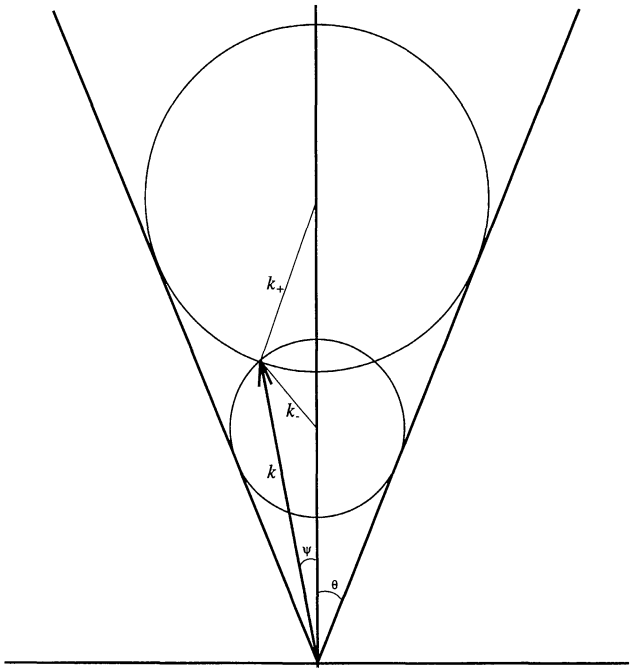

Figure C1. The build-up of the Fourier transform $H(k,\psi)$ of the semi-konus density inside a cone with half-angle θ, by a weighted sum of spheres. At each point (k,ψ) with $\psi < \theta$ there are two spheres with radii k_+ and k_- that contribute to $H(k,\psi)$.

The function $H(\boldsymbol{k})$ can also be written as the Fourier transform of the semi-konus density, i.e.,

$$H(\boldsymbol{k}) = \int \mathrm{d}^3\boldsymbol{r}\, \rho_{\mathrm{sk}}(\boldsymbol{r}|\theta)\ \exp(-\mathrm{i}\boldsymbol{k}\cdot\boldsymbol{r}). \tag{C7}$$

Therefore, one has that

$$H(0,0,0) = \int \mathrm{d}^3\boldsymbol{r}\, \rho_{\mathrm{sk}}(\boldsymbol{r}|\theta) = M_{\mathrm{kon}}, \tag{C8}$$

where M_{kon} is the total mass of the semi-konus density.

The weight function we used to construct the generalized konus density is $g(k) = k^{\mu-1}\mathrm{e}^{-bk}$. Since $k_\pm \propto k$ we derive from equations (C6) and (C8) that

$$M_{\mathrm{kon}} = C \lim_{k\to 0} k^{\mu-2}[\mathrm{e}^{-bf(0)k} - \mathrm{e}^{-bg(0)k}], \tag{C9}$$

where C is a constant that depends on μ, b and θ, and f and g are functions of the angle ψ. Therefore, for $\mu = 1$ the total mass of the konus density is infinite. For $\mu = 2$ one has $M_{\mathrm{kon}} > 0$, but finite, and for $\mu > 2$ the total mass is equal to zero.

We now show that the higher order konus densities $\rho^n_{\mathrm{k}}(r,z|\theta)$ $(n \geq 2)$ of the generalized konus densities have zero total mass. Therefore we write the Fourier transform of the semi-konus density $\rho^n_{\mathrm{sk}}(r,z|\theta)$ as $H^n_b(\boldsymbol{k})$, where n denotes the order of the semi-konus density and b the scalelength. From equation (C6) it is straightforward to show that

$$H^1_b(a\boldsymbol{k}) = a^{\mu-2}H^1_{ab}(\boldsymbol{k}), \tag{C10}$$

where $a \geq 0$ is a constant, and $a\boldsymbol{k} = (ak,\psi,\phi)$. The Fourier transform of the second-order semi-konus density is the convolution of $H^1_b(\boldsymbol{k})$ with itself, i.e.,

$$H^2_b(\boldsymbol{k}) = \int \mathrm{d}^3\boldsymbol{k}'\ H^1_b(\boldsymbol{k}-\boldsymbol{k}')\ H^1_b(\boldsymbol{k}'). \tag{C11}$$

Then

$$H^2_b(a\boldsymbol{k}) = \int \mathrm{d}^3\boldsymbol{k}'\ H^1_b(a\boldsymbol{k}-\boldsymbol{k}')\ H^1_b(\boldsymbol{k}'). \tag{C12}$$

Since $\boldsymbol{k}'$ is a dummy variable of integration, we can substitute $\boldsymbol{k}' = a\boldsymbol{z}$ to find

$$\begin{aligned} H^2_b(a\boldsymbol{k}) &= a^3 \int \mathrm{d}^3\boldsymbol{z}\, H^1_b[a(\boldsymbol{k}-\boldsymbol{z})]\ H^1_b(a\boldsymbol{z}) \\ &= a^{2\mu-1} \int \mathrm{d}^3\boldsymbol{z}\, H^1_{ab}(\boldsymbol{k}-\boldsymbol{z})\ H^1_{ab}(\boldsymbol{z}) \\ &= a^{2\mu-1} H^2_{ab}(\boldsymbol{k}). \end{aligned} \tag{C13}$$

From equation (C13) we see that whereas $H^1_b(\boldsymbol{k}) \propto k^{\mu-1}$ at small radii, we find that $H^2_b(\boldsymbol{k}) \propto k^{2\mu-1}$ at small radii. From this analysis it is clear that the total mass $M_{\mathrm{tot}} = H^n_b(0,0,0)$ is equal to zero for $n \geq 2$.

This paper has been typeset from a TEX/LATEX file prepared by the author.